Cavitation of Polyethylene during Extrusion Processing Instabilities*

YOUNGGON SON, KALMAN B. MIGLER

National Institute of Standards and Technology, Polymers Division, 100 Bureau Drive, Stop 8544, Gaithersburg, Maryland 20899

ABSTRACT: We present observations of cavitation that occur inside a capillary die during extrusion of polyethylene. This phenomenon was observed over the last 1.5 mm of the capillary tube immediately upstream of the exit. We observed spontaneous formation of voids near the wall that grew to a typical length and width of 150 μm, and then shrank and disappeared over a time frame of approximately 20 ms. From velocity measurements of these structures, we concluded that their width in the radial direction was smaller than in the axial and lateral directions, and they were near the wall. The shape of the cavities was highly irregular. We assessed the roles of extensional stress and shear stress at the exit region and concluded that they were not the direct cause of cavitation. Rather, cavitation occurs in conjunction with an upstream rupture of the polymer that occurs in the contraction region leading into the capillary tube (gross melt fracture). We argue that the exit region does, however, serve as the initiation point of the cavitation because of a combination of the reduced pressure and extensional stress. © 2002 Wiley Periodicals, Inc. J Polym Sci Part B: Polym Phys 40: 2791–2799, 2002

Keywords: extrusion; processing; polyolefins; cavitation; gross melt fracture

INTRODUCTION

The production rate of many polymer-extrusion processes such as fiber spinning, film blowing, and wire coating is limited by extrusion instabilities. In an extrusion process, when the throughput exceeds a critical value, small-amplitude periodic distortions appear on the surface of the extrudate (known as surface melt fracture or sharkskin melt fracture). These periodic distortions are regular in frequency and amplitude. As the throughput increases, these take the more severe form of larger irregular distortions [gross melt fracture (GMF) or wavy fracture]. GMF typically involves diameter variations of 10 % or more. GMF occurs in many classes of materials including both linear and branched morphologies.[1]

Much research has been done on sharkskin melt fracture (SMF) because it occurs at relatively low throughput. It is now generally accepted that SMF originates in the die exit region. On the other hand, GMF has received less attention. Major contributions regarding the features and causes for GMF were made in the late 1950s and 1960s.[2] GMF is initiated at the die entrance where the melt undergoes uniaxial extension as a result of the flow contraction. Important visualization studies (tracer technique and flow birefringence) in the entrance region are reported in the early literature.[3–6] According to these results, at the onset of GMF the converging lamella flow pattern at the entrance becomes disturbed, the flow profile fluctuates, and the axial symmetry of the streamline vanishes. As the flow rate increases further, the melt at the centerline of the entrance region fractures; the asymmetry and

fluctuations propagate to the capillary die and consequently result in the chaotic appearance of the extrudate. We term this behavior *upstream rupture*. This behavior looks similar to the turbulent flow of a nonelastic liquid. However, this turbulent-like flow pattern for a polymer melt occurs at a very low Reynolds number and is believed to be caused by the elastic nature of the polymer melt. This is why GMF is often called *elastic turbulence.*[7] GMF occurs when the extensional stress at the entrance of the die exceeds a critical condition that depends mainly on the polymeric fluid and little on the die diameter, length, and die material.[8] Kim and Dealy[8] demonstrated that a critical tensile stress estimated from the entrance pressure drop can serve as a universal criterion for the onset of GMF. They also investigated the effect of molecular structure on the critical tensile stress with several polyethylenes. They suggest that the critical tensile stress is independent of molecular weight for constant polydispersity but increases with an increase in the long chain branching and polydispersity.[9]

A separate line of research concerns cavitation in fluids where examples are found in disparate fields such as sonoluminescence[10] and atomization of liquid jets.[11] Joseph[12] argues that cavitation (sometimes called voids) is a cohesive fracture that occurs when the stress in the material exceeds a critical tensile stress. In polymeric materials, cavitation has been observed by direct visualization in simple shear flow when the stress exceeds a critical value for the cases of polystyrene and polybutadiene.[13] In the former case, it was shown that the failure is cohesive.

Despite the fact that the stress fields during pressure-driven extrusion are significant, there have been no experimental reports of cavitation during polymer processing. In a numerical model, Tremblay[14] predicted the stress profile of a fluid in a capillary die. He found that the stress could become negative near the exit region for the fluid near the wall-air-polymer three-phase line. He conjectured that the negative stress gives rise to cavitation, which is then the cause of the sharkskin surface melt fracture, described previously.

In this work, we report an intriguing cavitation phenomenon that was observed during extrusion of a linear low-density polyethylene (LLDPE). We used real-time high-speed video microscopy to capture the growth and dissolution of these voids as the polymer was extruded through a transparent sapphire die. The occurrence of cavitation in the die exit region is always accompanied by the upstream rupture of the melt. We describe several experiments that discern the relative importance of shear stress, extensional stress, and upstream instabilities as possible causes of the cavitation.

EXPERIMENTAL

Materials

The two materials investigated are commercially available LLDPEs. Both polymers are metallocene catalyzed. One is Resin A, characterized by a melt index of 1.0 g/10 min and a density of 0.87 g/cm^3. The other is Resin B, characterized by a melt index of 1.2 g/10 min and a density of 0.90 g/cm^3. These two materials were chosen because their flow instability behaviors are rather different from each other.

Apparatus and Method

In this work, we used a sapphire capillary die situated at the exit of a Haake[15] twin-screw extruder, as described by Migler et al.[16] Briefly, a microscope with stroboscopic illumination is constructed at the die exit to image the flow inside the capillary. Particle-tracking velocimetry with a high-speed video camera (1000 frames/s) attached to a microscope was used to measure the velocity profile of the polymer melt inside the capillary. The length and the radius of the capillary were 32 and 0.8 mm, respectively. Experiments were conducted at 160 and 180 °C and at various throughputs ranging from 1 to 25 g/min.

In one set of experiments, a fluoro-polymer-coated sapphire tube was used to investigate its effect on GMF and cavitation. Only the inner wall near the exit (from the die exit to ca. 2 mm upstream) was coated. The coating involved repetitive introduction of a dilute mixture (1% mass fraction of fluoropolymer) of acetone and Dynamar FX9613 into a hot die (160 °C) and the subsequent evaporation of the acetone. The coated fluoropolymer achieved good adhesion with the sapphire die upon heating to 180 °C for several minutes.

Upstream Rupture Visualization

The apparatus described previously images the flow in the exit region of the tube but not in the upstream region where the polymer flow lines converge into the tube. As this region is known to

be the site of the initiation of GMF, we needed to correlate the downstream cavitation observations with the upstream flow behavior. Thus, we performed a rupture visualization experiment in a different device, a Gottfert Rheo-Tester 2000[15] capillary rheometer (12-mm barrel diameter). This visualization technique has been used to measure entrance flow instabilities.[3,8] A carbon black (CB) filled sample was prepared by extruding the mixture of polymer + CB (0.5% mass fraction) into a cylindrical form of approximately 11.5 mm diameter followed by cutting the rod into a disc of 2 mm thickness. Discs of polymer without CB were also prepared in the same way. The discs were loaded into the barrel of the capillary rheometer equipped with a tungsten carbide die of 1 mm diameter and 30 mm length. One CB-filled disc was inserted for every neat polymer disc as shown in Figure 1. The extrudates obtained from the rupture experiment at various conditions were investigated under an optical microscope in transparent mode at 2× magnification.

RESULTS AND DISCUSSION

The flow curve (ΔP vs flow rate) of Resin A from an extrusion run is illustrated in Figure 2 and

Figure 2. Flow curves of Resin A at two different temperatures. The data were taken from a low shear rate to a high shear rate. The standard uncertainty (one standard deviation) is less than 5%.
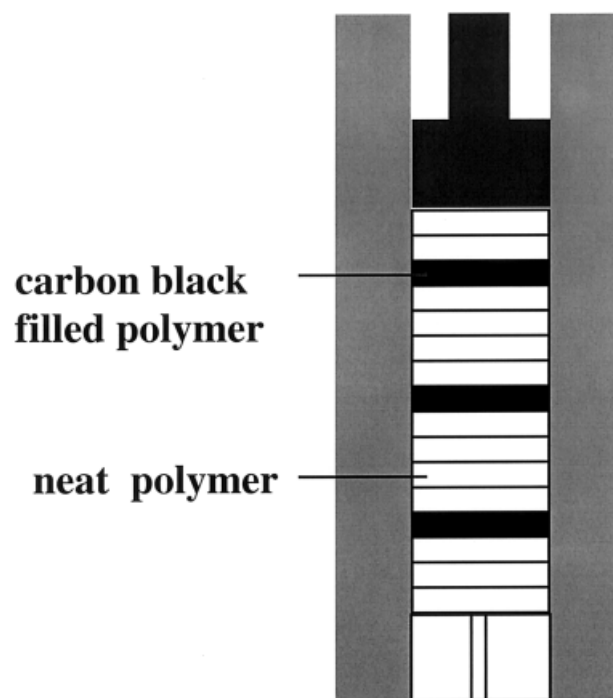

Figure 1. Method for loading discs into the barrel of the capillary rheometer for the upstream rupture-visualization experiment. The diameter of the barrel is 12 mm. The thickness of each disk is 2 mm.
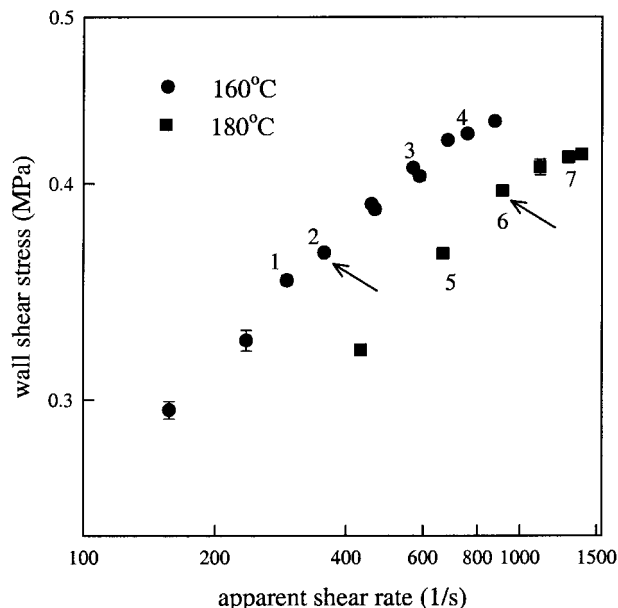
Figure 3 portrays photographs of the extrudate identified by the numbers in Figure 2. The arrows in Figure 2 indicate the onset of GMF determined by the appearance of the extrudate, that is, severe and chaotic distortion. Because the focus of this study is on the GMF regime, we do not show data for the stable flow regime where the extrudate has a smooth and glossy surface. In fact, the extrudate produced at the minimum flow rate available in our extruder at a temperature of 160 °C still revealed the sharkskin defect. The onset of SMF for 180 °C is about 1 g/min. A stick-slip or spurt-flow regime accompanied by a typical flow-curve discontinuity is not observed for Resin A (but is observed for Resin B).

Below the throughput for the onset of GMF, the extrudate surface shows a typical sharkskin texture, that is, a small amplitude and high-frequency disturbance (numbers 1 and 5 in Fig. 3). Above the onset of GMF, the appearance of the extrudate changes dramatically, characterized by its wavy, rough, and chaotic nature. In the GMF regime, a striking phenomenon is observed—transient cavitation in the die exit region. Figure 4 shows a typical example. The time interval between each micrograph is 1 ms. Initially (not shown here), only flowing LLDPE is observed in the capillary. Then, a black spot appears (1 ms) whose size grows rapidly as seen in the next mi-
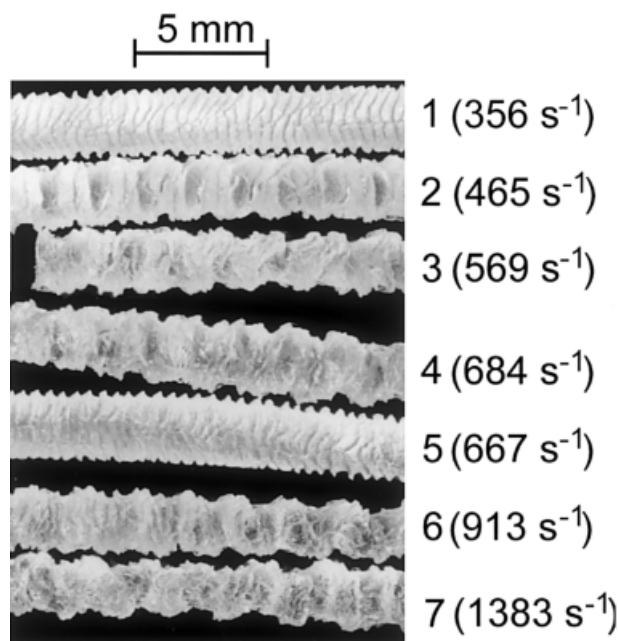
Figure 3. Extrudates obtained under various processing conditions. Numbers in each photo correspond to those in Figure 2. The diameter of the capillary die used is 1.58 mm.

crograph (2 ms). The size of the cavity reaches a maximum at about 5 ms after its creation and then decreases relatively slowly until it vanishes completely. The lifetime of most cavities ranges from 20 to 25 ms. The shape of the cavities is highly irregular, and its maximum size varies from several tens of microns to about 150 μm in width and length.

The cavities are easily visualized because there is a strong difference in the index of refraction between the polymer ($n = 1.5$) and that of the cavity ($n = 1.0$). Over several years of various types of experiments with extrusion visualization,[17–19] we never observed this phenomenon, only in this case of extrusion during GMF. The robustness of the effect, its time kinetics, its behavior to changes in shear and extensional flow, and its similar appearance to cavitation in shear flow[13] all lead us to conclude that these observations are real and not the result of an optical artifact.

Two separate observations demonstrate that the cavities form at or near the wall. First, Figure 5 exhibits optical micrographs for various cavities when the optical focal plane is varied from the wall to a plane 300 μm above the wall. The cavities are most clearly seen when the focal plane is at the wall; the image becomes progressively blurred as the focal plane moves away from it.

This indicates that the cavity exists at the capillary wall or very close to it. Second, the velocity profiles in Figure 6 show complementary information. At the lower flow rate the polymer sticks at the wall (velocity goes to zero), whereas at the higher flow rate it slips. In both cases the velocity of the cavity indicates that it is located at the wall (or within 50 μm from it). We can conclude from the velocimetry that the cavity width is less than 50 μm, which means that the size of the cavity in the radial direction (flow-gradient direction) is less than that in the flow or vorticity directions.

Figure 7 describes the average cavity size at various processing conditions. We plotted the average area of the cavities in the flow-vorticity plane. Cavitation becomes more severe as the throughput increases and the temperature decreases. Figure 8 shows the average size of the cavities at various axial positions from the die exit. We observe that cavitation occurs (0.5–1.5) mm upstream of the exit, depending on experimental conditions. The cavitation frequency, that is, how many times the cavitation occurs per unit
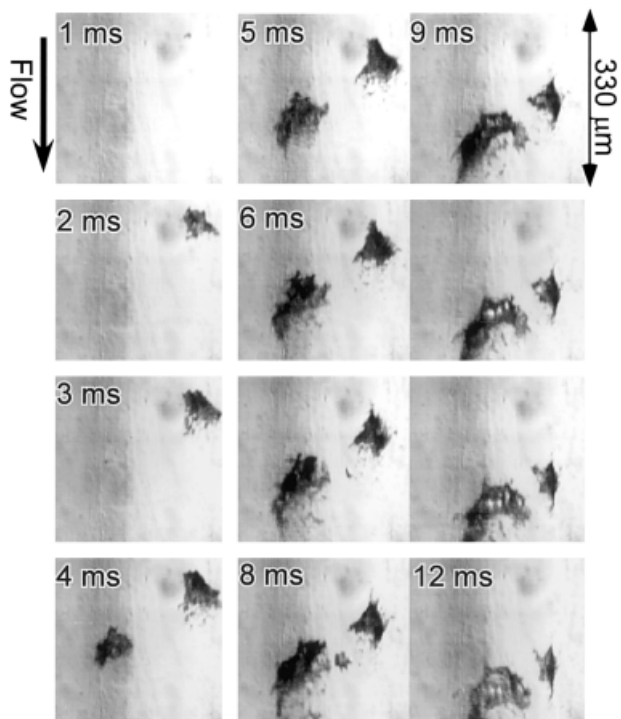

Figure 4. Example of formation and extinction of the cavity. Extrusion conditions for this set of micrographs correspond to number 3 in Figure 1. Time difference between successive micrographs is 1 ms. Each individual micrograph is in the same location; the bottom of each micrograph is approximately 30 μm upstream from the die exit.
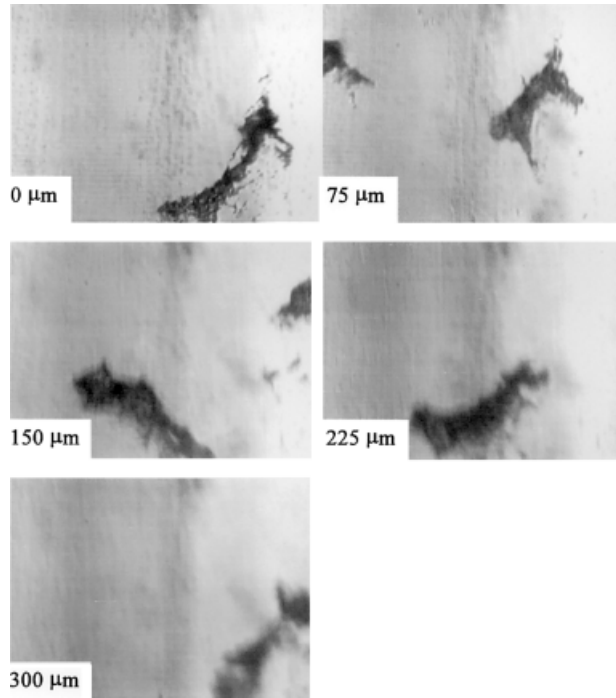
Figure 5. Optical micrographs for the cavitation where the focal plane is translated with respect to the wall. Each individual micrograph is in the same (z,θ) location, but the focal plane is different; the bottom of each micrograph is approximately 30 μm upstream from the die exit (extrusion temperature: 160 °C; apparent shear rate: 465 s^{-1}, and wall shear stress: 386,000 Pa).
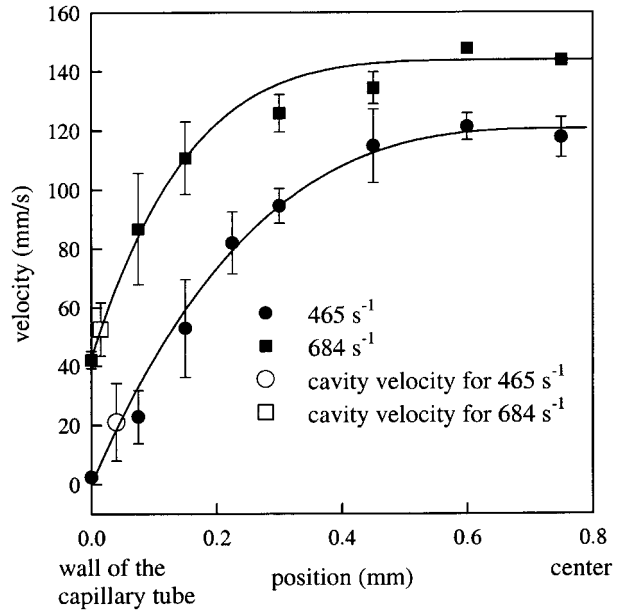

Figure 6. Velocity profile of the polymer melt inside the capillary tube and cavity velocity at two different screw speeds. The curves are best fit to a three-parameter power-law model with slippage ($V = V_s + V_o[1 - (r/R)^{1 + 1/n}]$, where V is the velocity at the tube wall, V_o is the velocity at the center, and n is the power-law index. The bracket on each data point represents an uncertainty of one standard deviation (extrusion temperature: 160 °C).

period of time, shows these same trends (in terms of throughput, area, and position) as that for the area. Thus, the intensity of cavitation is most intense at the die exit and decreases progressively with increasing upstream distance from it.

To assess the cause of cavitation we first consider the role of extensional and shear stress. It is known that the stress field spikes in the exit region. The surface layer accelerates from rest (stick at the wall) to the extrudate velocity at the die exit.[20] This is the main source for the generation of the extensional flow field in the vicinity of the die lip of the exit region. The fact that the cavitation increases with increasing throughput and decreasing melt temperature implies that the shear and/or extensional stress level plays an important role in this phenomenon. As described previously, both shear stress[13,21] and extensional stress[12] can produce cavitation in a polymer melt when the induced stress is greater than the cohesive force of the polymer melt.[22] The fact that the cavity exists near the wall (where shear stress is greatest) further implicates shear stress as the

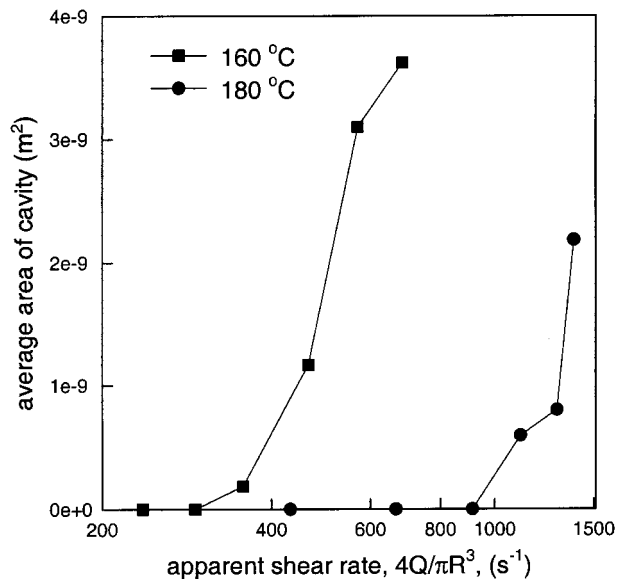**Figure 7.** Average area of the cavity versus apparent shear rate. The location for the cavitation is up to 330 μm from the die exit. The standard uncertainty (one standard deviation) is less then 10%.
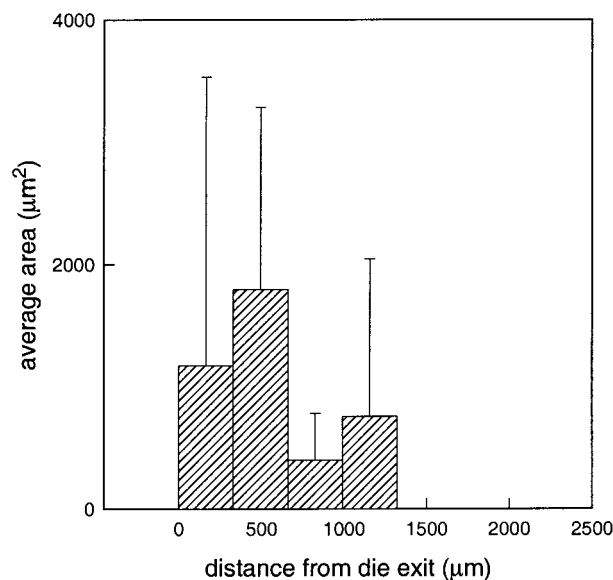
Figure 8. Average area of the cavity versus distance from the capillary exit. Top of bracket indicates the largest values at a given position (extrusion temperature: 160 °C, apparent shear rate: 465 s^{-1}, and wall shear stress: 386,000 Pa). The standard uncertainty is 10%.

causative parameter. An additional argument for the importance of shear stress is the similarity in appearance between our cavities and those found by Archer et al.[13] in a simple shear experiment. In their case, cavitation is observed when the polymer flows over an uncleaned silica surface and is believed to be caused by surface heterogeneities—the polymer slips in one region and sticks in an adjacent one.

However, we believe that shear and extensional stress is not the causative factor. First, when we coated the die exit (up to ~ 2 mm upstream) with the fluoropolymer, the onset of GMF and cavitation phenomenon are not changed (i.e., they are still observed). The fluoropolymer diminishes polymer adsorption and allows significant wall slip that decreases the extensional and shear stress in the die exit region.[16,23] This observation differs from that of Archer et al.[13] (simple shear) in which cavitation disappears in the presence of a fluoropolymer coating.

Second, we observe that the radial position of the cavitation is not (or little) affected by an increase in the throughput or decrease in the temperature. If the shear stress were the dominant factor for the cavitation, the thickness of the zone, where cavitation occurs, would be wider with an increase in throughput or a decrease in temperature, that is, the increase in the shear stress.

The fact that the cavitation zone extends up to 1.5 mm upstream from the die exit makes us doubt that extensional stress at the die exit is the direct cause for the cavitation. A numerical calculation predicted that the extensional flow is significant within several micrometers from the die exit.[14] Migler et al.[19] observed that the polymer melt approaching the die exit near the capillary wall does not accelerate (up to 30 μm upstream of the exit). This is also what we observe in this study (measurements not shown). These observations suggest that the shear stress (as well as the extensional stress) at the die exit does not play a direct role.

We performed an additional experiment in which we modify the flow by placing an obstacle in front of the die exit. We found that no cavitation occurs even at very high throughput. In this case, the surface of the extrudate is much smoother than it is during GMF, showing only small-scaled roughness (ripplelike shape). We return to this observation subsequently.

Now we assess the relationship between cavitation and the other well-known flow instabilities. It has been well documented that the entrance region plays a critical role for the onset of GMF. We observe that cavitation always occurs in the GMF regime for Resin A. Therefore, we speculate that the rupture of the polymer melts in the die-entrance region cause the cavitation phenomenon. To verify this speculation, we carried out a rupture-visualization experiment (with colored discs) in the capillary rheometer and compared the rupture experiment with the cavitation observed in the twin-screw extrusion experiment. Figure 9 shows a flow curve of Resin A obtained via batch capillary rheometry with the flow curve by twin-screw extrusion (the same experiment as shown in Fig. 2). The flow curve obtained from the capillary rheometer matches that from the twin-screw extruder. Figure 10 displays micrographs of selected extrudates from the rupture-visualization experiment. Black lines or black dots inside the extrudates correspond to the portion of CB-labeled polymer (and are thus a streamline). The micrograph taken at 10 s^{-1} (apparent wall shear rate) shows that the streamline is very stable and that the outer surface is very smooth. As the flow rate increases, SMF is observed. In the micrograph taken at 100 s^{-1} wall shear rate, the streamline is still continuous although the outer surface of the extrudate indicates a typical sharkskin texture. The streamline is continuous up to the highest flow rate that does not show the GMF. Above the critical shear rate, marked by "onset of
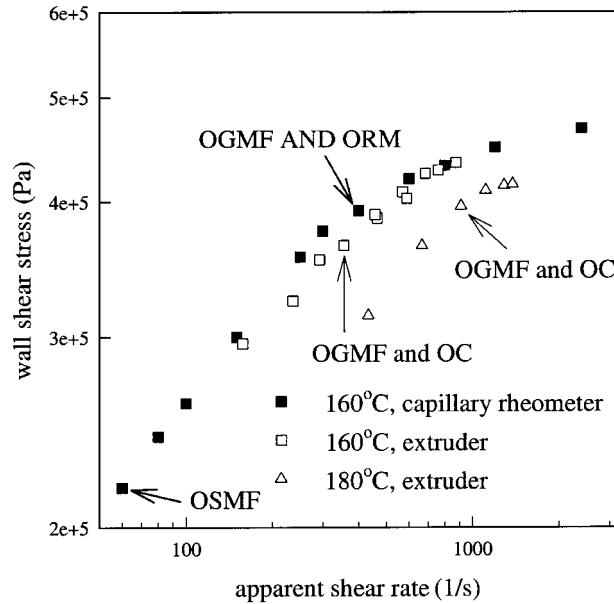
Figure 9. Flow curves of Resin A from capillary rheometer (filled symbol) and extruder (open symbol). OSMF: onset of sharkskin melt fracture, OGMF: onset of gross melt fracture, ORM: onset of upstream rupture of melt, and OC: onset of cavitation phenomenon. The standard uncertainty is less than 5%.

Figure 11. Flow curves of Resin B from capillary rheometer (filled symbol) and extruder (open symbol) at 160 °C. OSMF: onset of sharkskin melt fracture, OGMF: onset of gross melt fracture, ORM: onset of upstream rupture of melt, and OC: onset of cavitation phenomenon.

gross melt fracture" (OGMF) and "onset of the rupture of the melt" (ORM) in Figure 10, GMF is observed. Here GMF refers to the distorted profile of the extrudate, and ORM refers to the breakup of the streamlines in the entrance region as seen by the black-labeled polymer. In the GMF regime, CB-labeled polymer is broken into discontinuous pieces as shown in Figure 10 (800 s^{-1}). In Resin A, the cavitation phenomenon is always accompanied by the upstream rupture of the melt because
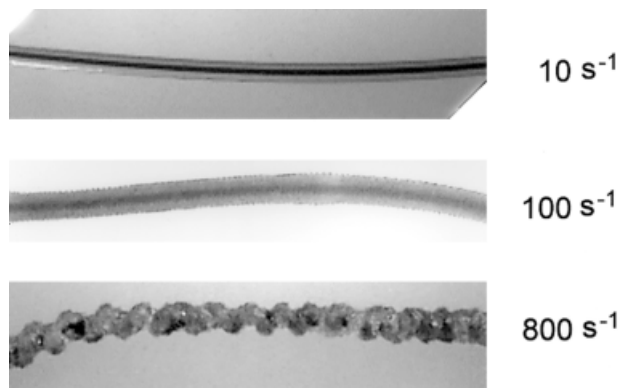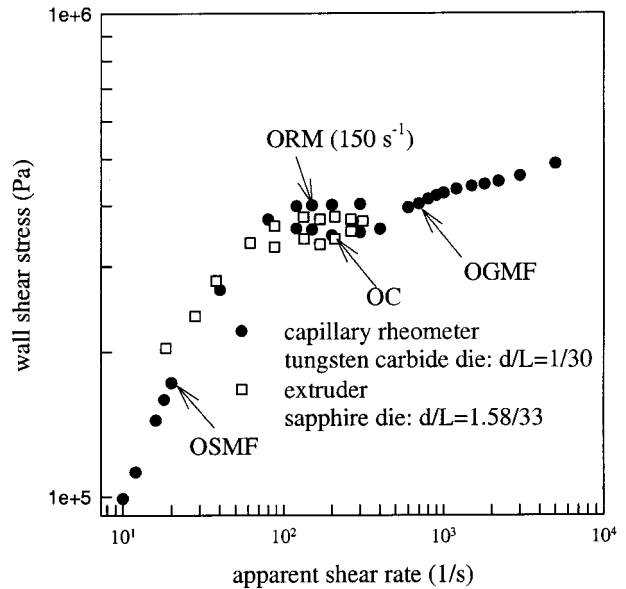

Figure 10. Extrudates of Resin A obtained from the capillary rheometer under various shear rates at 160 °C.

the cavitation (in the extrusion) and the discontinuity of the streamline (in the capillary rheometer) are always accompanied by GMF in Resin A.

We also investigate the flow characteristics of Resin B under twin-screw extrusion and during capillary rheometry. Figure 11 depicts flow curves of Resin B at 160 °C by both capillary rheometry and a twin-screw extrusion experiment. It exhibits a somewhat different flow behavior than Resin A. A typical behavior of a linear polyethylene melt is seen, that is, stable flow followed by unstable flow (stick-slip flow) above a critical shear rate (ca. 120 s^{-1} for the capillary rheometer and ca. 100 s^{-1} for the extrusion). Because of experimental limitations, the maximum shear rate for the twin-screw extrusion is about 300 s^{-1}. Up to this shear rate, GMF is not observed. However, the cavitation phenomenon is nevertheless observed for the Resin B above the shear rate of 210 s^{-1} as denoted by "onset of cavitation phenomenon" (OC) in Figure 11. The characteristics of the cavitation observed in Resin B extrusion are very similar with that of Resin A. The difference between these two polymers is that the cavitation for Resin A is always accompanied by the GMF, but that of Resin B is not.

Figure 12 portrays photographs of extrudates for Resin B from the upstream rupture-visualiza-
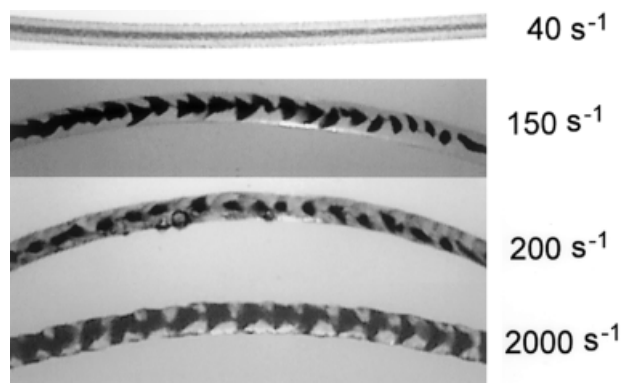
Figure 12. Extrudates of Resin B obtained from the capillary rheometer under various shear rates at 160 °C.

tion experiment at several selected shear rates. Below the shear rate of 150 s^{-1} the extrudate shows a normal sharkskin feature. However, above the shear rate of 150 s^{-1} the streamline is broken into the discontinuous pieces for the portion of slip among the stick-slip extrudate. Above the shear rate of 800 s^{-1} as marked by OGMF, the extrudate exhibits a typical characteristic for the GMF. Apparently, the cavitation phenomenon observed in the extrusion and the discontinuity of the streamline (upstream rupture of the melt) observed in the capillary rheometer accompany each other because the shear rate for the onset of both phenomena is very similar for Resin B. Thus for the Resin B sample, the upstream rupture occurs at a lower shear rate than GMF, whereas for other reported polymers they occur at the same shear rate. Therefore, we can say that the cavitation coincides with the upstream rupture, not the GMF.

The concurrence of downstream cavitation with upstream melt rupture in two materials with different modes of flow instability indicates that these two phenomena are intimately connected. We conjecture that unstable, chaotic, and fractured flow at the entrance is the cause or seed of the cavitation at the die-exit region. As described in the introduction, the melts fracture at the entrance to the die during GMF. The polymer is under pressure in this upstream region (typically 30 MPa to 50 MPa). This pressure prevents cavitation although the tensile stresses may otherwise be strong enough to produce it. However, as the melt then approaches the exit of the die, the pressure drops to that of the atmosphere. If the upstream rupture of the melt has not healed by the time the melt reaches the die exit, then we speculate that the stress on the ruptured polymer

may open a cavity. At the die exit, there is also extensional stress (although weaker in the presence of a fluoropolymer coating). We speculate that the combination of the reduced pressure at the exit coupled with the increase in extensional stress initiates the cavitation event. In the presence of the obstacle (which eliminates cavitation), the flow path of the polymer is lengthened so that the polymer is still under pressure at our point of observation. Additionally, the obstacle greatly reduces the extensional stress because the velocity discontinuity at the die exit disappears in the presence of the obstacle as a result of its gently expanding flow pattern. Thus, the forces to initiate the cavitation are not present in the experiments with the obstacle. A remaining question concerns the possible role of absorbed volatile gases that may nucleate to form bubbles under the conditions of stress as a possible cause of the cavitation. We feel that because we observe both formation and subsequent shrinkage of the cavities that such a picture would require the gases to quickly reabsorb into the polymer, although the pressure decreases as the material moves toward the exit. Thus, we do not believe that the cavitation is due to gas-bubble nucleation.

Tremblay[14] suggests that sharkskin may be the result of a cavitation event. He showed numerically that a large negative pressure can exist at the die exit by simulating the flow of a linear polydimethylsiloxane melt using a finite-element program. However, we observe the cavitation to occur only at a throughput well beyond the onset of sharkskin. We conclude that his suggestion does not explain the observations in this work.

CONCLUSIONS

The cavitation phenomenon is observed in an LLDPE extrusion process. We observe cavitation in the first 1.5 mm upstream of the exit at high flow rate, where we observe the upstream rupture of the melt. We see cavities at the wall form (seemingly out of nothing) grow to a length and width of about 150 μm and then shrink down and disappear. From velocity measurements of these structures, we conclude that their width in the radial direction is very thin as compared with its width in the axial and lateral directions and that they are in contact with the wall. The process for the growth and disappearance is approximately 20 to 25 ms. The cavitation occurs only at throughputs where

the rupture of the melt at a die-entrance region is observed. From these facts, we conclude that the cavitation phenomenon is closely related to the melt fracture at the die entrance.

REFERENCES

1. Denn, M. M. Annu Rev Fluid Mech 2001, 33, 265–287.
2. Tordellar, J. P. Unstable Flow of Molten Polymers. In Rheology; Eirich, F. R., Ed.; Academic: New York, 1969; Vol. 5, Chapter 2, pp 57–92.
3. Bagley, E. B.; Birks, A. M. J Appl Phys 1960, 31, 556–561.
4. Cook, N. P.; Furno, F. J.; Eirich, F. R. Trans Soc Rheol 1965, 9, 405–420.
5. Tordellar, J. P. Trans Soc Rheol 1957, 1, 203–212.
6. Tordellar, J. P. J Appl Polym Sci 1963, 7, 215–229.
7. Petrie, C. J. S.; Denn, M. M. AIChE J 1976, 22, 209–236.
8. Kim, S.; Dealy, J. M. Polym Eng Sci 2001, 42, 482–494.
9. Kim, S.; Dealy, J. M. Polym Eng Sci 2001, 42, 495–503.
10. Putterman, S.; Evans, P. G.; Vazquez, G.; Weninger, K. Nature 2001, 409, 782–783.
11. Tamaki, N.; Shimizu, M.; Hiroyasu, H. Atomization Sprays 2001, 11, 125–137.
12. Joseph, D. D. J Fluid Mech 1998, 366, 367–378.
13. Archer, L. A.; Ternet, D.; Larson, R. G. Rheol Acta 1997, 36, 579–584.
14. Tremblay, B. J Rheol 1991, 35, 985–998.
15. Certain equipment, instruments, or materials are identified in this article to adequately specify the experimental details. Such identification does not imply recommendation by the National Institute of Standards and Technology nor does it imply the materials are necessarily the best available for the purpose.
16. Migler, K. B.; Lavallee, C.; Dillon, M. P.; Woods, S. S.; Gettinger, C. L. J Rheol 2001, 45, 565–581.
17. Migler, K. B.; Hobbie, E. K.; Qiao, F. Polym Eng Sci 1999, 39, 2282–2291.
18. Migler, K. B. J Rheol 2000, 44, 277–290.
19. Migler, K. B.; Son, Y.; Qiao, F.; Flynn, K. J Rheol 2002, 46, 383–400.
20. Cogswell, F. N. J Non-Newtonian Fluid Mech 1977, 2, 37–47.
21. Chen, Y. L.; Larson, R. G.; Patel, S. S. Rheol Acta 1994, 33, 243–256.
22. Hutton, J. F. Nature 1963, 200, 646–648.
23. Piau, J. M.; Kissi, N.; Mezghani, A. J Non-Newtonian Fluid Mech 1995, 59, 11–30.